FERMILAB-CONF-422-TD
ACCEPTED

Overview of the Quench Heater Performance for MQXF, the Nb_3Sn low-β Quadrupole for the High Luminosity LHC

S. Izquierdo Bermudez, G. Ambrosio, H. Bajas, N. Bourcey, G. Chlachidze, J. Ferradas Troitino, P. Ferracin, J. C. Perez, F-O. Pincot, E. Ravaioli, C. Santini, S. Stoynev, E. Todesco, G.L. Sabbi, G. Vallone

(Invited Paper)

***Abstract*— In the framework of the High-Luminosity upgrade of the Large Hadron Collider, the US LARP collaboration and CERN are jointly developing a 150 mm aperture Nb_3Sn quadrupole for the LHC interaction regions. Due to the large stored energy density and the low copper stabilizer section, the quench protection of these magnets is particularly challenging, relying on a combination of quench heaters attached to the coil surface and CLIQ units electrically connected to the coils. This paper summarizes the performance of the quench heater strips in different configurations relevant to machine operation. The analysis is focused on the inner layer quench heaters, where several heater strips failed during powering tests. Failure modes are discussed in order to address the technology issues and provide guidance for future tests.**

***Index Terms*— High Luminosity LHC, Quench Protection, High Field Nb_3Sn Magnet.**

I. Introduction

THE upgrade of the LHC aims at increasing the integrated luminosity by a factor ten beyond its nominal performance expected for 2023 [1]. Part of the upgrade relies on the replacement of the single aperture quadrupoles in the interaction region (the low-β or inner triplet quadrupoles). The magnet, named as MQXF, consists in a 150 mm aperture quadrupole based on Nb_3Sn technology [2]. Protection is particularly challenging due to the high stored energy density (130 MJ/m^3) and the low copper stabilizer fraction (55 %). The energy has to be uniformly dissipated upon quench detection within 0.3 s in order to maintain the peak temperature and voltage within the acceptable limits [3]. Main magnet and conductor parameters relevant for protection are summarized in Table I.

TABLE I. Main Magnet And Conductor Parameters.

Parameter	Unit	Q1/3	Q2a/b
Strand diameter	mm	0.850 ± 0.003	
Number of strands	--	40	
Copper/non-Copper ratio	--	1.2 ± 0.1	
Nominal operational current (I_{nom})	kA	16.47	
Conductor peak field at I_{nom}	T	11.41	
Differential inductance at I_{nom}	mH/m	8.21	
Strand energy density at I_{nom}	MJ/m^3	130	
Strand current density at I_{nom} (J_{eng})	A/mm^3	726	
Magnetic length	m	4.20	7.15

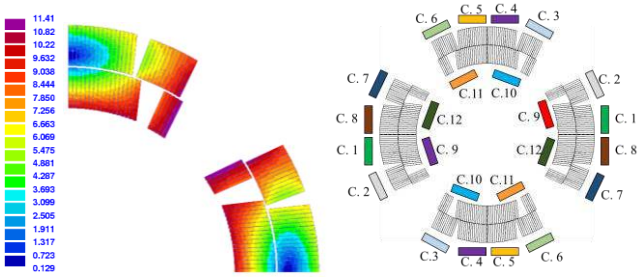

Fig. 1. Cross section of one coil, showing the magnetic field in Tesla at nominal current (16.47 kA) (Left). Schematic of the quench heater circuits per magnet (Right).

The quench protection system of these magnets will include a combination of quench heaters attached to the coil surface and CLIQ units electrically connected to the coils [7]. Every coil is equipped with four outer layer and two inner layer heater strips, connected in series as shown in Fig 1(right), leading to twelve heater circuits per magnet. This paper summarizes the quench protection heaters performance of the tested short model magnets (MQXFS) ([4]-[6]). Scalability of the heater has been demonstrated after measuring similar heater delays in 1.2-m-length and 4-m-length coils tested in mirror configuration [7].

Manuscript receipt and acceptance dates will be inserted here. This work was supported by the High Luminosity LHC Project at CERN and by the DOE through the U.S. LHC Accelerator Research Program.

S. Izquierdo Bermudez, H. Bajas, N. Bourcey, P. Ferracin, J. Ferradas Troitino, E. Todesco, J. C. Perez, F-O. Pincot and G. Vallone are with CERN, 1211 Geneva, Switzerland (e-mail: susana.izquierdo.bermudez@cern.ch).

G. Ambrosio, G. Chlachidze, C. Santini, and S. Stoynev are with Fermi National Accelerator Laboratory (FNAL), Batavia, IL 60510 USA.

G.L. Sabbi and E. Ravaioli are with Lawrence Berkeley National Laboratory (LBNL), Berkley, CA 94720 USA.

Color versions of one or more of the figures in this paper are available online at http://ieeexplore.ieee.org.

Digital Object Identifier will be inserted here upon acceptance.

TABLE II. QUENCH HEATER CIRCUIT POWERING PARAMETERS FOR OPERATION CONDITIONS IN HL-LHC.

		Outer Layer		Inner Layer	
		Q1/3	Q2a/b	Q1/3	Q2a/b
Resistance	Ω	2.9	4.6	4.2	6.7
Capacitance	mF	7.05	7.05	7.05	7.05
Voltage t = 0 s	V	570	900	565	900
Current t = 0 s	A	198	198	134	134
Time constant	ms	20	32	30	47
Max. Power density HS	W/cm^2	213	213	98	98
Energy density HS	J/cm^2	2.16	3.42	1.45	2.32

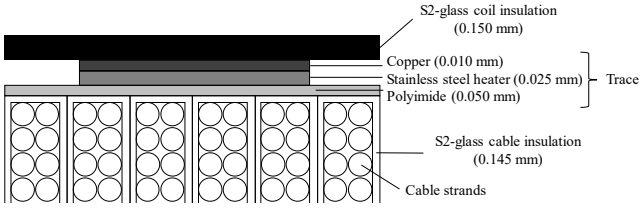

Fig. 2. Schematic view of the cable, trace and coil insulation.

Outer layer quench heaters performed as expected, demonstrating an adequate and reliable performance. Several cases of electrical failures and heater to coil detachments were identified during MQXFS1 and MQXFS3 test campaigns, which question the long-term reliability of the inner-layer quench heaters. Failure modes and inspection results are discussed in order to address the technology issues and provide guidance for future tests. In the third short model, MQXFS5, inner layer quench heaters were not powered in the first and second thermal cycles in order to assess the integrity of the heaters after cool down and magnet powering. Heater protection studies in MQXFS5 will be performed in the future.

II. QUENCH HEATER DESIGN AND FABRICATION

MQXF quench heaters are composed by 25 µm stainless steel strips (AISI 304), bonded to a 50 µm layer of polyimide in the so-called trace. The trace is positioned on the inner and outer surface of the reacted coil, and it is covered by a layer of glass before coil impregnation (see Fig. 2). In an attempt to reduce the detachment of the inner layer heaters from the coil experienced in previous LARP magnets [8], the polyimide of the trace is perforated. The physical limits when designing the heaters are the temperature and the maximum voltage from heater to coil. In the case of MQXF, the maximum acceptable temperature on the heaters under adiabatic conditions was set to 350 K and the peak voltage to ± 450 V. In order to reduce the overall strip resistance and limit the heater voltage, the stainless steel is plated with 10 µm of copper. The pattern is defined to maximize the number of turns covered by heater stations (HS) and to quench the conductor between stations in less than 5 ms. The copper sections in the inner layer heaters are narrower to maximize the area of perforated polyimide (see Fig 3). Table II summarizes the heater powering parameters for the 4.2 m and 7.15 m length magnets.

The production of the heaters relies on the printed circuit board technology. A 10-µm layer of copper is electroplated to the stainless steel-polyimide base material with a 0.3 µm layer of nickel over the stainless steel surface to improve the copper

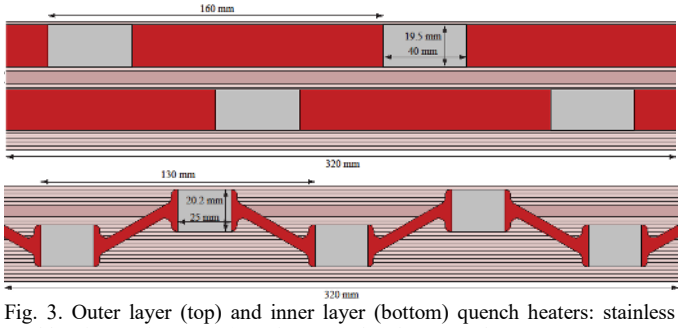

Fig. 3. Outer layer (top) and inner layer (bottom) quench heaters: stainless steel heating stations (gray), and copper plated parts (red).

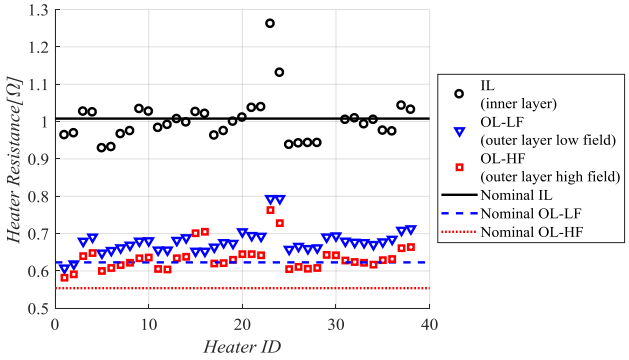

Fig. 4. Measured quench heater resistance at room temperature for the short model coils. IL = Inner layer, OL = Outer layer, HF = High field, LF = Low field

to steel adhesion. The Residual Resistivity Ratio (RRR) of the deposited copper ranges from 25 to 40. Copper, stainless steel and nickel is then removed through chemical etching with the required heater pattern. A second etching of the copper defines the final geometry of the heater stations. The last step is to perforate and polish the trace in order to improve the adhesion during coil impregnation and to improve the cooling during magnet operation. The dielectric strength of the polyimide at the end of the process is verified applying a DC voltage of 3 kV under a local pressure of less than 1 MPa. Fig. 4 summarizes the measured heater resistance in the short model coils and compares it to the nominal resistance.

The insulation resistance from heater to coil is verified after coil impregnation and magnet assembly applying a DC voltage of 2.5 kV. Based on the latest quench protection analysis [9], the test voltage was increased to 3 kV in summer 2017. All short model coils (22 produced by CERN, 9 produced by LARP) passed the test after coil manufacturing. The only exception is CERN coil 102, which shows a weak coil to end-shoe and end-shoe to heater electrical insulation. The source of the problem was a default on the heater powering wires. The insulation resistance limit was verified for the first CERN and LARP practice coils, showing a good heater to coil insulation up to 5 kV.

After coil impregnation and at different stages of the magnet assembly, quench heaters are subjected to a discharge test. The peak current in the discharge test is 80 A and the deposited energy is 23 J. This test is only performed on CERN magnets and no failures were identified to date.

TABLE III. QUENCH HEATER CIRCUIT POWERING PARAMETERS FOR THE TESTED SHORT MODEL MAGNETS.

MQXF magnet ID		Outer Layer S1	Outer Layer S3	Inner Layer S1	Inner Layer S3
Resistance (R)	Ω	1.69	6.00	2.48	6.00
Capacitance (C)	mF	19.2	7.05	19.2	7.05
Voltage t = 0 s (V)	V	331	900	331	900
Current t = 0 s (I)	A	196	150	133	150
Time constant (τ)	ms	32	42	48	42
Power density HS (P_d)	W/cm^2	209	123	97	123
Energy density HS (E_d)	J/cm^2	3.39	2.59	2.31	2.59

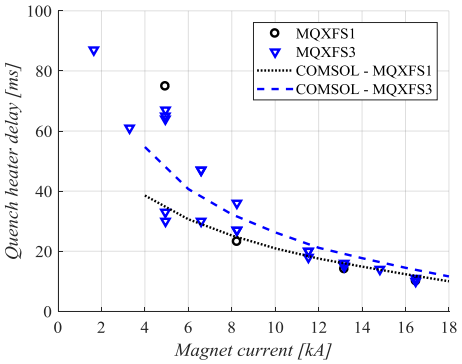

Fig. 5. Quench heater delay as a function of the magnet current for the outer layer high field coil block.

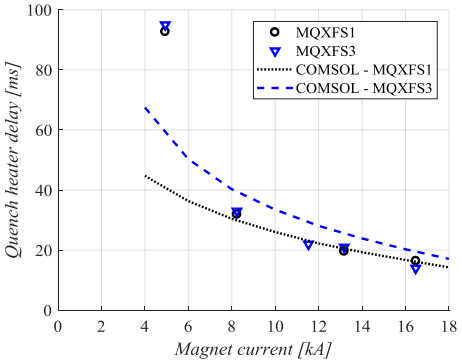

Fig. 6. Quench heater delay as a function of the magnet current for the outer layer low field coil block.

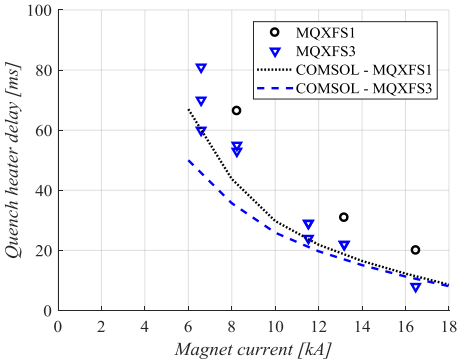

Fig. 7. Quench heater delay as a function of the magnet current for the inner layer.

III. QUENCH HEATER PERFORMANCE

The role of the heaters is to induce a fast and distributed quench to quickly discharge the magnet current. The main concerns are the delay needed to induce a quench and the quench propagation within the coil. Heater powering parameters are adapted for the short models to be as close as possible to the 7.15 m length magnet ones, compatible with the hardware limitations in the magnet test facility. The aim is to have a peak power density in the heater station ($P_d = RI^2/A_{HS}$) and an energy density deposited during the heater current decay ($E_d = P_d\tau/2$) representative of the operation conditions (R is the heater resistance, I is the heater peak current, A_{HS} is the contact surface between heater station and coil, and τ is the time constant of the exponential heater current decay). Table III summarizes the heater powering parameters for the tested short models magnets.

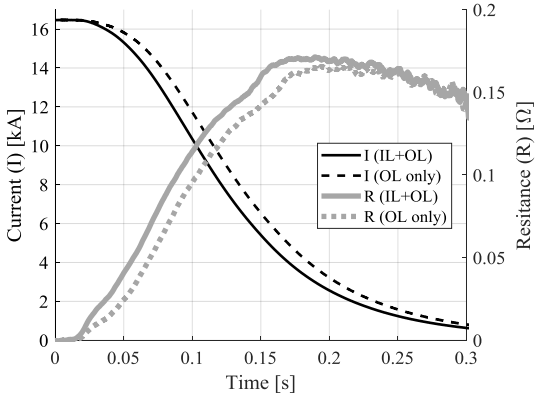

Fig. 8. Current decay and magnet resistance growth in MQXFS3 as a function of time for a discharge firing inner layer and outer layer heaters (IL+OL) or only outer layer heaters (OL only).

A. Quench heater delays

Quench heater delay is defined as the time between the heater powering and the start of a resistive transition in the coil. The measured delays in MQXFS1 and MQXFS3 as a function of the magnet current are plot in Fig. 5, 6 and 7. At nominal operating current, outer layer heater delays are 2 to 5 ms shorter than predicted by the COMSOL model [10] for MQXFS3 and in agreement with expectations in MQXFS1. The heater powering conditions used in the model are summarized in Table III. Larger spread is observed for the inner layer heaters, where measured and modelled delays are within 10 ms at nominal magnet current. At lower current level, the discrepancy between model and measurements increases, in particular for the outer layer low field and inner layer heaters. Due to the larger margin in terms of protection at low current, the longer measured delays in the range of 4 to 8 kA are not considered an issue for the magnet protection. Measurements are consistent in MQXFS1 and MQXFS3 for the outer layer heaters. Inner layer heaters in MQXFS1 were around 10 ms slower than in MQXFS3. According to the model, smaller difference on the inner layer heater delays in between the two magnets is expected.

B. Quench integral studies

To study the current decay, quench propagation and resistance build up in the magnet, quench heater discharge test are systematically done at different current levels using the heater firing parameters defined in Table III. Quench detection system is manually triggered, activating the quench protection heaters. The opening of the energy extraction switch is delayed by 1000 ms. Figure 8 shows the measured current

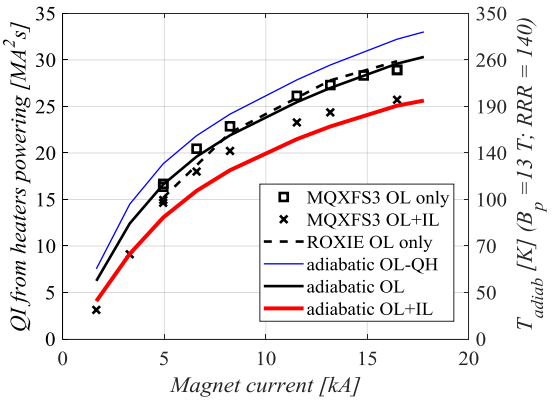

Fig. 9. Quench integral as a function of the magnet current. Secondary y-axis (not in scale) shows the adiabatic hot spot temperature on the conductor assuming a peak field of 13 T and RRR of 140.

decay and resistance growth for the quenches at nominal current in MQXFS3 magnet. Time equal to zero corresponds to the moment the heaters are powered. The case where inner layer and outer layer heaters are powered is compared to the case where only the outer layer heaters are protecting the magnet. Three out of the eight inner layer quench heater strips failed before these tests so they were not powered during the quench integral studies. The average coil temperature at the end of the decay is 100-120 K.

A conservative estimate of the hot spot can be obtained by using the heat balance equation assuming adiabatic conditions and constant magnetic field equal to the peak field in the conductor:

$$\int_0^{\infty} [I(t)]^2 \, dt = A_{total} A_{Cu} \int_{T_0}^{T_\infty} \frac{C_p^{ave}(T)}{\rho_{Cu}(T)} \, dT \qquad (1)$$

where I is the current in the magnet, A_{total} the cross sectional surface of the cable (including insulation), A_{Cu} is the copper surface, C_p^{ave} the average volumetric specific heat and ρ_{Cu} the copper resistivity. The left-hand side depends only on the response of the circuit (what we call quench integral (QI)) and the right-hand side depends only on the materials in the cable. Figure 9 shows the measured quench integral in MQXFS3 discharges as a function of the magnet current. MQXFS1 discharges are not reported here since half of the coils were equipped with non-standard heaters [11], meaning that results cannot be directly extrapolated to the full-length magnets. The secondary y-axis shows the corresponding adiabatic temperature assuming a peak field of 13 T and a RRR equal to 140. Outer layer only heater discharges were performed twice at nominal current, showing excellent reproducibility (difference in quench integral among tests lower than 0.2 %). In the case of a natural quench occurring in the magnet, the actual quench load would be higher due to the additional time required to detect (~ 5 ms), validate the quench (~ 10 ms) and fire the heaters (~ 1-4 ms). At nominal current, this contribution is about 5 MA^2s (~ 70 K).

A zero-order approximation (0D) of the effectiveness of the heaters can be done by comparing the measured quench load with the expected value assuming that the magnet is fully or partially quenched at the minimum heater delay. Figure 9 shows the expected quench load for the case only the turns in contact with the outer layer heaters are quenched (OL-QH), all the outer layer turns are quenched (OL) and the case the magnet is fully quenched (OL+IL). The simulated QI using ROXIE-2D model [12], which includes the electro-magnetic and thermal transients occurring during the quench, is also plotted. As it can be seen in the graph, in spite of the heater failures (see section IV), inner layer heaters efficiently contribute to a faster discharge of the magnet current, in particular at high magnet current. A reduction of the hot spot temperature of 60-80 K at nominal current is expected thanks to the use of inner layer heaters. Even if the zero-order approximation relies on very crude assumptions, it provides a first good estimation of the quench integral. The measured difference in the quench integral for the OL only and OL+IL case is close to the 0D estimations. ROXIE model is close to the measured values, in particular at high current.

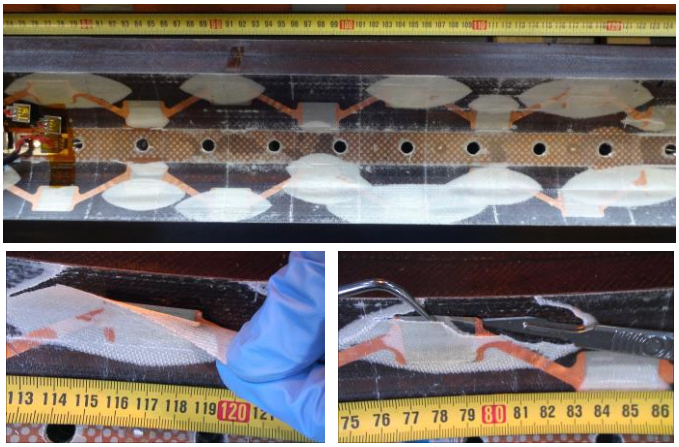

Fig. 10. View of the inner surface of LARP coil 7 after cold powering test (top). Example of the lack of adherence glass-epoxy to trace (left). Example of heater to polyimide delamination (right).

IV. Inner Layer Quench Heaters Failures

Whereas outer layer heaters operate under a compression force, supported by the collars, there is no pressure between the structure and the inner layer heaters. A series of modifications were implemented in the inner layer heater design in order to overcome the detachment of the heaters from the coil experienced in previous LARP magnets [8] (see section II). Despite the actions taken, Fig. 10 (top) shows the strong signs of delamination ("bubbles") on the inner coil diameter after powering test. Detachments where observed on all the coils, mostly located on the heater stations. Destructive inspection of LARP coil 7 revealed that the source of the problem is the epoxy to metal adherence and not the gluing of the trace to the coil turns, as it can be seen in Fig. 10, left. Heater to polyimide delamination (see Fig. 10, right) was only present in three out of the 38 heater stations in coil 7.

The current understanding is that superfluid helium penetrates into small voids within the epoxy. The increase of temperature during quench vaporizes the helium, generating high-pressure pockets, which delaminate the epoxy-glass matrix from the heater. The trace to conductor insulation (see Fig. 2) adherence is stronger, and no delamination is visible.

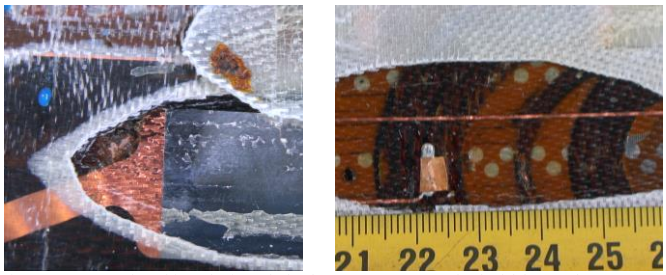

Fig. 11. Example of insulation default consequence of a bubble on the magnet straight section (left). Example of insulation default consequence of a bubble on the coil end (right).

Fig 12. LARP coil 7 before (left) and after (right) cold powering test.

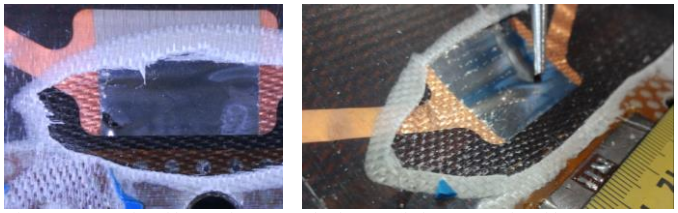

Fig 13. Example of burned spot on the heater (left). Example of heater to polyimide defect (right).

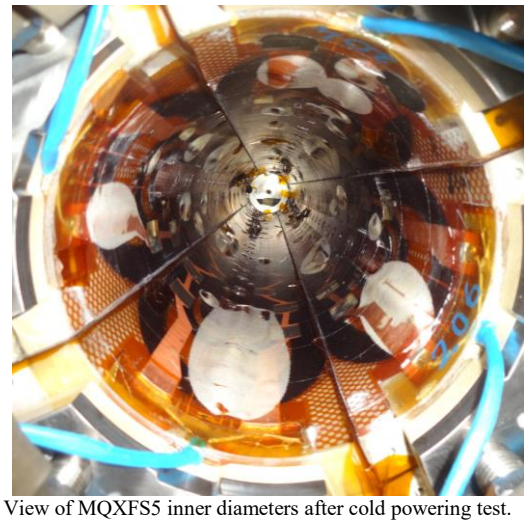

Fig. 14. View of MQXFS5 inner diameters after cold powering test.

Short model coils with different glass and trace layouts are under construction in order to understand if the problem can be partially solved. The highest risk of these bubbles is a degradation on the coil insulation since exposed conductor was observed in two locations, one on the magnet straight section (see Fig. 11, left) and one on the coil ends (see Fig. 11, right). Coil discharge test up to 4.5 kV did not show any electrical weakness.

The bubbles are not only over the heater stations, but also in the coil ends. Figure 12 shows a view of the inner surface of LARP coil 7 before and after cold powering test. In order to study the bubble formation in absence of inner layer quench heaters, a coil where the trace is not installed in the inner

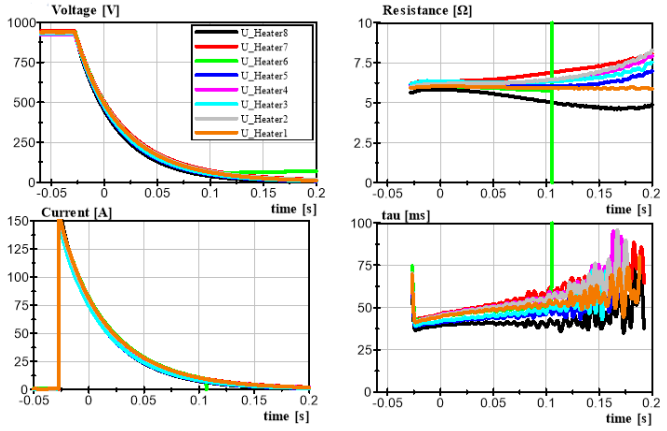

Fig. 15. Quench heater discharge curves during the failure (at t ~ 0.1 s) on the straight part of coil 106 inner layer heater.

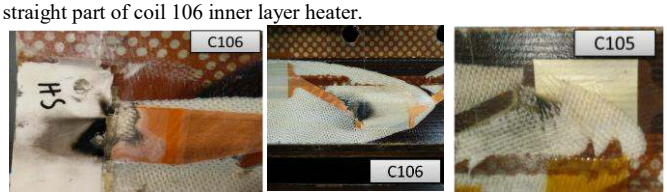

Fig. 16. Quench heater failures during cold powering test in MQXFS3.

surface is under production. The post-mortem inspection of coil 7 also showed a burnt spot at the edge of one heater station (see Fig 13, left) and several locations with a bubble or fold underneath the heater station (see Fig. 13, right). Even if these specific heaters did not fail during cold powering test, long-term reliability is compromised.

Following the strong signs of delamination observed in MQXFS3, inner layer heaters in MQXFS5 were not powered in the first and second thermal cycles in order to decouple the effect of the heater powering and the magnet quench. Figure 14 shows a view of MQXFS5 bore after testing. Bubbles are present in the inner coil surface, mainly on the quench heater stations and the coil ends. This is a clear indication that the main source of the bubbles is the increase of the coil temperature during a quench and not the powering of the quench heaters.

During cold powering test, three out of the eight inner layer heaters installed in MQXFS3 failed. In MQXFS1, three inner layer heaters showed weak electrical insulation at cold (failures at 750 V with respect to the 1 kV target) and were never powered. Heater voltage and current are measured during cold powering test with ~ 10 kHz sampling frequency. Figure 15 shows as an example the heater evaluation tool, where the destruction of the heater is visible at the end of the decay in the measured voltage and current of the heater circuit.

Two different type of failures were identified in MQXFS3. The first type of failure (see Fig. 16, left) occurred at the level of the coil ends, in the region where the quench heater strip is soldered to the heater powering wire in the so-called “splice block soldering pocket”. The quench heater strip was too short with respect to the coil resulting in a mechanically weak assembly. Quench heater design was modified and this weakness is not present in the recent coils. The second type of failure was in the straight part of the quench heater. Two heater strips were lost due to this failure mode (see Fig 16,

TABLE IV
INSULATION VOLTAGE [KV] QUENCH HEATER TO COIL AFTER COLD POWERING TEST AT ROOM TEMPERATURE

		OL-HF		OL-LF		IL	
Mag.	Coil	R	L	R	L	R	L
S1	3	>1.0	>1.0	>1.0	>1.0	>1.0[3]	>1.0[3]
	5	>1.0	>1.0	>1.0	>1.0	>1.0[1]	>1.0
	103	>1.0	>1.0	>1.0	>1.0	>1.0	>1.0[1]
	104	>1.0	>1.0	>1.0	>1.0	>1.0	>1.0[1]
S3	7	>2.5	>2.5	>2.5	>2.5	<2.5	<2.5
	105	>2.5	>2.5	>2.5	>2.5	0.1[2]	0.1
	106	>2.5	>2.5	>2.5	>2.5	<2.5[2]	<2.5[2]
	107	>2.5	>2.5	>2.5	>2.5	0.5	>2.5
S5	203	Insulation test not performed after cold powering test				>1.0[3]	0.2[3]
	204					0.2[3]	>1.0[3]
	205					0.2[3]	>1.0[3]
	206					>1.0[3]	>1.0[3]

1. Did not pass electrical tests at 1.9 K, so never powered at 1.9 K.
2. Failed during powering test.
3. Heaters never powered at cold.

middle and right). The source of these failures could be related to a local defect on the quench heater strip during their fabrication or during assembly on the coils. Tests performed in the past with heater defects made on purpose revealed that the detection of a defect by monitoring the voltage is very difficult since the change on resistance is very small [13]. A second possible, and more likely, source of the failures on the straight part of the heaters is a damage on the strip following an epoxy-glass delamination.

Insulation tests up to 3 kV were performed between the coils and the protection heaters after cold powering test, both for the inner layer and outer layer strips. All outer layer quench heaters passed the insulation test at 1 kV (MQXFS1) and 2.5 kV (MQXFS3) with less than 1 μA leakage current. Outer layer heaters in MQXFS5 were not verified after cold powering test. The aim was to minimize the risks in MQXFS5 before next thermal cycle, dedicated to protection studies and magnetic measurements. Inner layer heaters have shown weaker electrical insulation after cold powering test, as summarized in Table IV. In MQXFS1, all the heaters passed the 1 kV electrical insulation test after cold test. In MQXS3, seven out of eight heaters failed the 2.5 kV insulation test. All inner layer heaters failed the test at 3 kV in MQXFS5, with a breakdown voltage from 2.6 to 2.9 kV. The test was repeated in MQXFS5 at 1 kV, with a failure of 3 out of the 8 heaters at 200 V. The rest of the inner layer heater strips in MQXFS5 passed the 1 kV test.

V. CONCLUSIONS

The quench heater performance of the Nb_3Sn quadrupole magnets for the high luminosity upgrade was assessed on relevant LHC operation conditions. Quench heaters are able to quench a large portion of the coil in a sufficiently short time, in agreement with expectations. No failures were identified in the outer layer heaters of the short model magnets, demonstrating the maturity and robustness of the quench heater technology. About 30 % of the inner layer heater strips failed during powering test. In spite of the failures, the use of the inner layer heaters reduced significantly the quench integral at nominal current, with an expected decrease of the hot spot temperature of 60–80 K. The source of the failures is the glass-epoxy to heater delamination in the inner coil surface. Several coils are under production with different insulation and heater layout in order to solve the identified failure mode.

ACKNOWLEDGMENT

The authors wish to thank CERN and LARP technical staff for the construction of the magnets, and CERN's, FNAL's Test Facilities for the cold powering tests.

REFERENCES

[1] I. Bejar Alonso, L. Rossi, "HiLumi LHC Technical Design Report" CERN-ACC-2015-0140. Year 2015.
[2] P. Ferracin, *et al.*, "Magnet design of the 150 mm aperture low-β quadrupoles for the high luminosity LHC," *IEEE Trans. Appl. Supercond.*, vol. 24, no. 3, Jun. 2014, Art. ID 4002306.
[3] G. Ambrosio, "Maximum allowable temperature during quench in Nb_3Sn accelerator magnets," in Proceedings, WAMSDO 2013 Workshop on Accelerator Magnet, Superconductor, Design and Optimization: CERN Geneva, Switzerland, 15-16 Jan 2013, 2013, pp. 43–46. https://inspirehep.net/record/1277941/files/arXiv:1401.3955.pdf
[4] G. Chlachidze, et al., "Performance of the first short model 150 mm aperture Nb_3Sn quadrupole MQXFS for the High-Luminosity LHC upgrade," IEEE Trans. Appl. Supercond., vol. 27, no. 4, pp. 1–5, 2017.
[5] S. Stoynev et al., "Summary of test results of MQXFS1 - the first short model 150 mm aperture Nb_3Sn quadrupole for the high-luminosity LHC upgrade," *IEEE Trans. Appl. Supercond*., submitted for publication.
[6] H. Bajas et al., "Test results of the short models MQXFS3 and MQXFS5 for the HL-LHC upgrade," *IEEE Trans. Appl. Supercond*., submitted for publication.
[7] E. Ravaioli, *et al.*, "Quench Protection System Optimization for the High Luminosity LHC Nb_3Sn Quadrupole," *IEEE Trans. Appl. Supercond*., vol. 27, no. 4, pp. 4001705, Jun. 2016.
[8] G. Ambrosio, *et al.,* "Test Results of the First 3.7 m Long Nb_3Sn Quadrupole by LARP and Future Plans," *IEEE Trans. Appl. Supercond*., vol. 21, no. 3, pp. 1858-1862, June 2011.
[9] E. Ravaioli, et al., "Quench protection studies for the high luminosity LHC inner triplet circuit", CERN Internal Report, EDMS 1760496.
[10] S. Izquierdo Bermudez, et al., "Quench Protection Studies of the 11-T Nb3Sn Dipole for the LHC Upgrade," *IEEE Trans. Appl. Supercond*., vol. 26, no. 4, pp. 4701605, 2016.
[11] G. Ambrosio and al., "MQXFS1 Quadrupole Fabrication Report," Tech. Rep. 2016.
[12] https://cern.ch/roxie
[13] M. Bajko, G. Berard, G. Rolando, G. Molinari, "Report on Quench Heater Failures", EDMS 889445, AT-MCS-Technical Note, 2008